

Demonstration of Multi-Hz repetition rate x-ray lasers at shorter wavelengths

J. J. Rocca^{*,a,b}, A. Rockwood^a, Y. Wang^b, S. Wang^b, M. Berrill^{b,c}, V. N. Shlyaptsev^b, H. Bravo^b, C.S.Menoni^b

^aPhysics Department, Colorado State University, Fort Collins, Co 80525; ^bElectrical and Computer Engineering Department, Colorado State University, Fort Collins, Co 80525; ^cOak Ridge National Laboratory, Oak Ridge, TN 37831

ABSTRACT

Compact, repetitively fired, gain-saturated x-ray lasers have been limited to wavelengths above $\lambda=8.85$ nm. Here we discuss their extension to $\lambda = 6.85$ nm by transient traveling wave excitation of Ni-like Gd ions in a plasma created with an optimized pre-pulse followed by rapid heating with an intense sub-ps pump pulse. Isoelectronic scaling also produced strong lasing at 6.67 nm and 6.11 nm in Ni-like Tb, and amplification at 6.41 nm and 5.85 nm in Ni-like Dy.

1. INTRODUCTION

Plasma-based x-ray lasers allow many experiments requiring bright, high energy, x-ray laser pulses to be conducted in compact facilities [1]–[5]. These lasers provide extremely monochromatic radiation, typically $\Delta\lambda / \lambda = 3 \times 10^{-5}$ [6], and when injection-seeded can reach full spatial and temporal coherence [7]–[9]. The efficient generation of high energy x-ray laser pulses requires operation in the gain-saturated regime. In this regime stimulated emission can extract the majority of the energy stored in the population inversion[10]. Gain saturation in plasma-based x-ray lasers was demonstrated for wavelengths as short as 5.8 nm at large laser facilities [11], [12]. However, these results required pump pulse energies on target larger than 70 J, which limited the repetition rate to a few shots per hour. Alternatively, transient table-top lasers [13], [14] pumped by picosecond laser pulses at grazing incidence [15], [16] require much less energy and can operate at repetition rates of typically 5-10 Hz at wavelengths as short as 10.9 nm[17]. The repetition rate of these lasers was recently increased to 100 Hz using pump lasers pumped by laser diodes [18], and 400 Hz operation was very recently reported at $\lambda= 18.9$ nm in Ni-like Mo [19]. However, the extension of practical plasma-based x-ray lasers that can fire repetitively to sub-10 nm wavelengths is challenging. Alessi et al. used laser pump pulse energies of up to 7.5 J on target to extend table-top, repetitive 1 Hz transient collisional soft x-ray amplification down to 7.36 nm[20]. Nevertheless, gain saturated operation was limited to a shortest wavelength of 8.85 nm in Ni-like La. A more recent experiment conducted in Ni-like Sm using a Nd: glass pump laser capable of firing a shot every 25 minutes was reported to approach gain saturation [21]. However, this could not be verified due to large pulse-to-pulse output pulse energy variations and the low repetition rate of the pump laser. In the case of the 6.85 nm line of Ni-like Gd gain was observed in a plasma pumped by 250 J pulses, but the amplification was far from reaching gain saturation [22].

Here we report the extension of gain saturated compact repetitive x-ray lasers down to 6.85 nm (181 eV) in Ni-like Gd. Furthermore, in the same experiments we observed gain at even shorter wavelength transitions, down to 5.85 nm (212 eV) in Ni-like Dy. The experiments were performed with a pump laser capable of firing at repetition rates up to 3.3 Hz[23].

2. EXPERIMENTAL SET UP AND METHODS

The x-ray lasers were excited with a sequence of two laser pulses from a $\lambda=800$ nm chirped pulse amplification Titanium:Sapphire (Ti:Sa) laser. The first pulse or pre-pulse consists of a longer pulse irradiating 1–2 mm thick solid slab target. This pulse ionizes the plasma to the vicinity of the Ni-like ionization stage. This is followed by a sub-picosecond pulse impinging at grazing incidence that rapidly heats the electrons to produce a transient population inversion by collisionally electron impact excitation. The experimental set up is shown in Fig. 1. For each pulse there were many parameters that were changes to maximise energy out of the x-ray laser. The intensity ratio of the pre-pulse to the sub-picosecond pulse was optimized using different beam splitters deflecting 30%, 40%, or 50% of the beam to be used as pre-pulse. Optimum pre-pulse plasma conditions were obtained using a 30% and 40 % for Sm and Gd respectively. This would

deliver 4.3 J and 6.9 J pre-pulse to the target for Sm and Gd respectively. The Ti:Sa pump laser has an acousto-optic programmable dispersive filter was used after the laser oscillator to tailor the bandwidth of the laser. This gives us the ability to adjust the length of the un-compressed pre-pulse from 45 ps to 300 ps to find the optimal conditions for laser amplification, which proved critical to obtain the results discussed below. It was found that the optimum pre-pulse duration is a FWHM duration of ~ 185 ps.

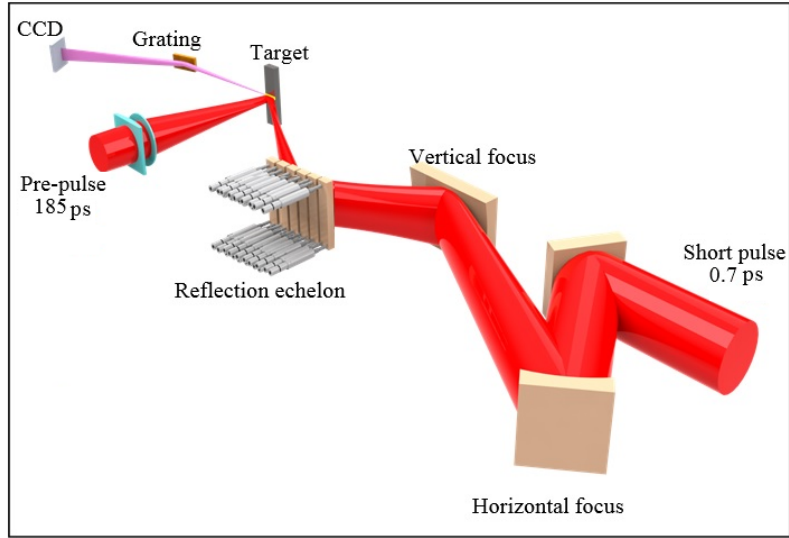


Figure 1. Experimental set up of the normal pre-pulse and with the short pulse with a grazing incidence respect to the target and the x-ray laser incident on a grating then to a CCD.

This is shown from Fig 2(a). The pre-pulse was focused onto the target using the combination of a spherical and a cylindrical lens to form a line focus of approximately $15 \mu\text{m}$ FWHM width and 9 mm or 10 mm length for Sm and Gd respectively. This gave a pre-pulse with intensities of $I \sim 1.7 \times 10^{13} \text{ W cm}^{-2}$ and $2.5 \times 10^{13} \text{ W cm}^{-2}$ on target for Sm and Gd respectively.

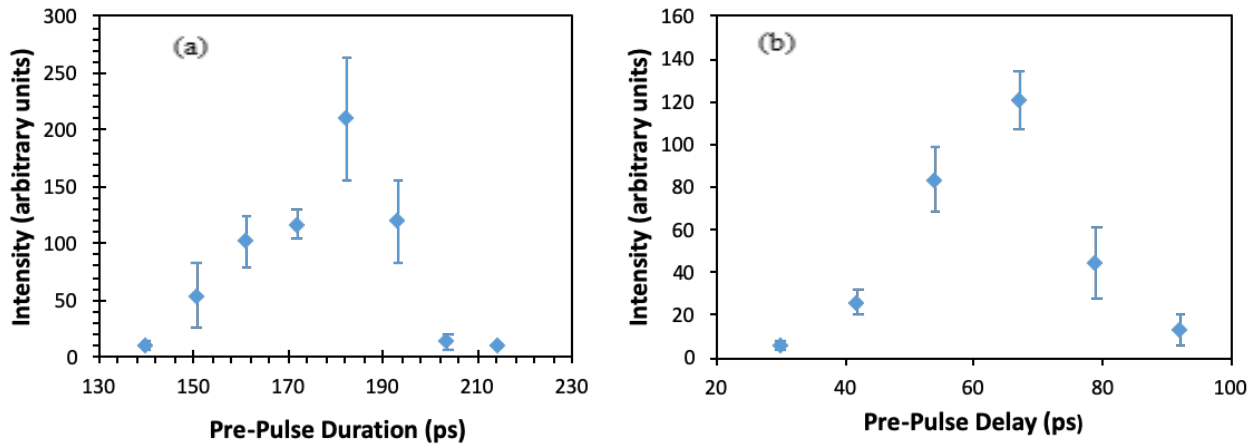


Figure 1. (a) Measured $\lambda=7.36 \text{ nm}$ laser intensity as a function of the pre-pulse duration. The points are the average of several laser shots and the error bar represents one standard deviation. (b) Measured laser intensity as a function of the delay between the peak of the pre-pulse and the peak of the short pulse. The plasma column length was 9 mm.

To achieve efficient pumping by the sub-picosecond pulse, we developed a focusing geometry designed to create a plasma column of constant width along the target. This focusing method, consisting of two cylindrical mirrors, is the same we

used previously to obtain gain-saturated lasing in Ni-Like La at 8.85 nm [21]. The plasma created by the pre-pulse is allowed to expand to reduce the density gradient and subsequently is rapidly heated with 7.1 J or 7.3 J pulse of a 0.7 ps FWHM duration for Sm and Gd respectively. The delay between the pre-pulse and the sub-picosecond pulse controls the plasma density and density gradient in the gain region, as well as the degree of ionization (fraction of Ni-like ions) at the time of excitation by the sub-picosecond pulse. Fig. 2(b) shows that the maximum laser output intensity is observed when the sub-picosecond pulse arrives at the target ~ 27 ps after the peak of the 185 ps FWHM pre-pulse. The sub-picosecond pulse is shaped into a line focus of approximately $30 \mu\text{m} \times 9 \text{mm} - 10 \text{mm}$ FWHM, corresponding to an intensity of $I \sim 3.5 - 3.7 \times 10^{15} \text{ W cm}^{-2}$ for Sm and Gd respectively. The target surface was tilted with respect to the axis of the sub-picosecond pulse to define a grazing incidence angle of 35 degrees or 43 degrees for efficient heating in the case of both Sm and Gd respectively. To optimize the incidence angle we changed the angle of the target respect to the short pulse beam and the position of the grating and CCD. Due to the short duration of the gain, the mismatch between the propagation velocities of the pump pulse and the amplified pulse significantly reduces the amplification of the x-ray laser pulse. To overcome this limitation, a reflection echelon [14], [24] composed of six adjustable mirror segments was used to obtain traveling wave excitation. The traveling wave velocity was adjusted for each new angle, and the focus was corrected for each angle for a traveling-wave excitation velocity of $(1.0 \pm 0.03)c$.

Gain measurements were conducted for both the Sm and Gd using single laser shots and moving the targets 1mm between shots. When the Gd laser was operated at 2.5-Hz repetition rate the target was translated at a speed of 2.5 mm s⁻¹ to renew the surface after each shot. The output of the x-ray lasers was analysed using a flat-field spectrometer with a nominally 1200-lines/mm variable space grating positioned at a grazing incidence angle of 3 degrees and a back-illuminated CCD detector placed at 48 cm from the target. The x-ray lasers pulse energies were estimated from the CCD counts taking into account the attenuation of the filters, the grating efficiency, and the quantum efficiency of the detector.

3. RESULTS

Strong amplification is observed in the $4d^1 S_0-4p^1 P_1$ transition at $\lambda = 7.36 \text{ nm}$ (169 eV) Ni-like Sm. Fig. 3(b) illustrates the Sm x-ray laser intensity grows by more than 3 orders of magnitude as the plasma column length increases from 3 mm to 8 mm. Saturation of the gain is observed to have an onset at a plasma-column length of approximately 5.5 mm. A fit of the data with an expression for the gain that takes into account saturation [25] yields a gain coefficient of 27.3 cm⁻¹ with a gain-length product of 16.6. The energy of the most intense Sm laser pulses was estimated to be $\sim 1.8 \mu\text{J}$ from the CCD counts, a value that is sufficient to perform single shot imaging [26].

Similar pre-pulse and sub-picosecond pulse conditions were used to obtain a gain-saturated 6.85 nm (181 eV) laser in Ni-like Gd. Fig. 3(a) shows a series of on-axis spectra as a function of the length for a Gd plasma column created from a polished Gd slab target with other irradiation parameters similar to those described above. Fig. 3 (c) shows the increase in the $\lambda = 6.85 \text{ nm}$ laser line intensity as a function of plasma column length. A fit to the data gives a gain coefficient of 26.3 cm⁻¹ and a gain length product of 16.2. The output pulse energy for the longest plasma column length is $\sim 1 \mu\text{J}$. Weak amplification was also observed for the $\lambda = 6.85 \text{ nm}$ line of Ni-like Sm and in the $\lambda = 6.33 \text{ nm}$ (196 eV) line of Ni-like Gd.

The demonstration of a gain-saturated tabletop laser at $\lambda = 6.85 \text{ nm}$ in Ni-like Gd at this reduced pump energy also opens the prospect for bright high-repetition-rate plasma-based lasers at shorter wavelengths. In progress toward this goal we made use of isoelectronic scaling along the elements of the lanthanide series to obtain lasing in several other shorter wavelength transitions from Ni-like ions. The spectra of Fig. 3 (b) show that the use of similar irradiation conditions for Ni-like Gd resulted in strong amplification in the $\lambda = 6.67 \text{ nm}$ (186 eV) and $\lambda = 6.11 \text{ nm}$ (203 eV) transitions of Ni-like Tb. Finally, we have also observed weak amplification in the $\lambda = 5.85 \text{ nm}$ (212 eV) and $\lambda = 6.41 \text{ nm}$ (193 eV) lines of Ni-like Dy (Fig. 4) using the same pump conditions. The spectra in Fig. 4 show that the intensity ratio of the longer wavelength to the shorter wavelength of the two J=0-1 lines becomes smaller as Z increases [27], with the shortest wavelength line becoming dominant for Ni-like Dy, as already observed in a normal incidence pumping experiment with much large laser pump energies [11], [28].

Fig. 5 shows the computed spatial distribution of the beam intensity as a function of plasma column length. The model simulations show that in the case of the higher Z-ions refraction shifts the maximum gain to the lower density region of $4 - 5 \times 10^{20} \text{ cm}^{-3}$. At this density the saturation intensity is computed to be $1.2 \times 10^{10} \text{ W cm}^{-2}$. Simulations show this intensity is reached after the rays travel $\sim 6 \text{ mm}$ along the plasma column axis. The output intensity is computed to exceed the saturation intensity by $> 3\times$ at the exit of the amplifier. Refraction is observed to shift the amplified beam progressively

away from the target and to decrease the output pulse energy. In absence of refraction simulations predict the laser pulse energy would be five to ten times the amount with refraction, potentially reaching $>10\mu\text{J}$.

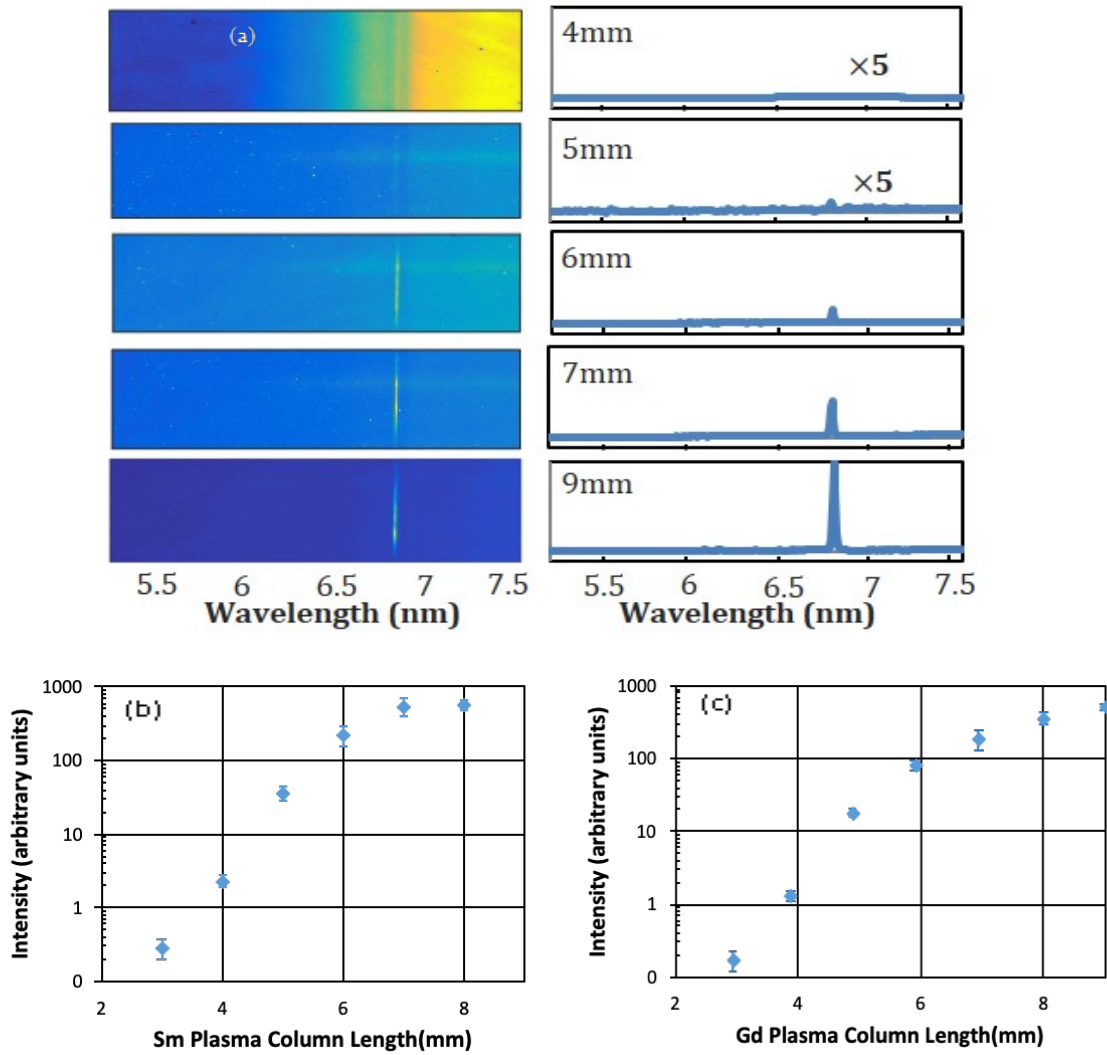


Figure. 3 (a) End-on spectra of a line-focus Gd plasma column showing saturated amplification in the $\lambda= 6.85$ nm line of Ni-like Gd. With the first two integrations plots on the right multiplied by 5. (b) Intensity of the $\lambda= 7.36$ nm laser line of Ni-like Sm as a function of the plasma-column length. The fit of the data yields a gain coefficient of 27.3 cm^{-1} and a gain-length product of 16.6. (c) Intensity of the $\lambda= 6.85$ nm laser line as a function of the plasma-column length. The fit of the data yields a gain coefficient of 26.3 cm^{-1} and a gain-length product of 16.2. The error bar represents 1 standard deviation.

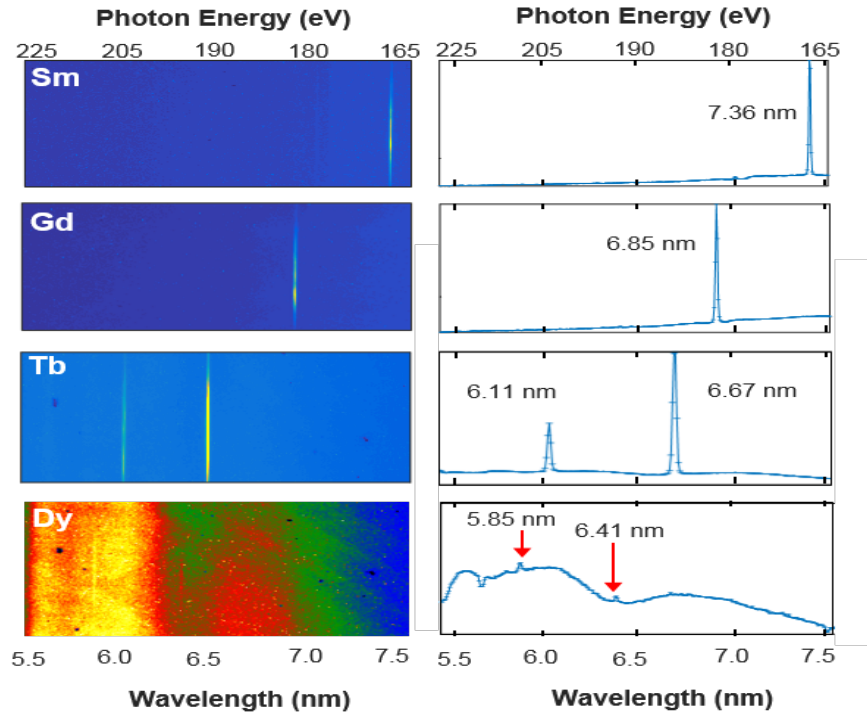


Figure. 4 End-on spectra showing lasing at progressively shorter wavelengths in the $4d^1 S_0-4p^1 P_1$ line of nickel-like lanthanide ions, down to $\lambda=5.85$ nm in nickel-like D.

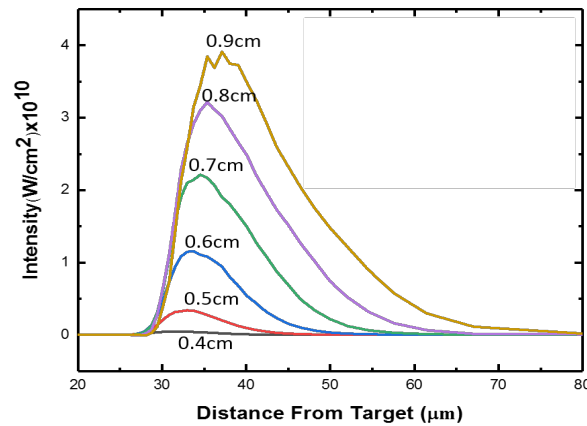


Figure. 5. Computed evolution of the intensity distribution of the x-ray laser beam of the 6.85 nm line of Ni-like Gd as function of plasma column length. (a) Intensity vs distance to the target for increasing plasma column lengths between 0.4 and 0.9 cm.

4. CONCLUSION

In conclusion, we have extended repetitively fired, compact, gain-saturated plasma-based lasers to the shortest wavelength to date: 6.85 nm. We have also observed laser amplification in other Ni-like lanthanide ions at wavelengths as short as 5.85 nm, opening the possibility of scaling table-top gain saturated lasers to even shorter wavelengths. The results will make possible applications requiring bright laser pulses with a large number of photons at these short wavelengths, such as single shot ultra-high resolution imaging of dynamic nano-scale phenomena to be realized at compact facilities.

Acknowledgements: Work supported by the U.S. Department of Energy, Office of Science, Basic Energy Sciences, under Award (DE-FG02-04ER15592).

REFERENCES

- [1] I. Kuznetsov, et al. *Nat. Commun.*, vol. 6, p. 6944, Apr. 2015.
- [2] G. Vaschenko, et al. *Opt. Lett.*, vol. 31, no. 9, pp. 1214–1216, May 2006.
- [3] R. F. Smith, et al. *Phys. Rev. Lett.*, vol. 89, no. 6, p. 65004, Jul. 2002.
- [4] F. Brizuela, et al. *Opt. Express*, vol. 18, no. 14, pp. 14467–14473, Jul. 2010.
- [5] R. Z. Tai, et al. *Phys. Rev. Lett.*, vol. 89, no. 25, p. 257602, Dec. 2002.
- [6] L. M. Meng, et al. *Opt. Express*, vol. 19, no. 13, pp. 12087–12092, Jun. 2011.
- [7] P. Zeitoun, et al. *Nature*, vol. 431, p. 426, Sep. 2004.
- [8] Y. Wang, et al. *Nat. Photonics*, vol. 2, p. 94, Jan. 2008.
- [9] Y. Wang, et al. *Opt. Lett.*, vol. 38, no. 23, pp. 5004–5007, Dec. 2013.
- [10] J. J. Rocca, *Rev. Sci. Instrum.*, vol. 70, no. 10, pp. 3799–3827, 1999.
- [11] R. Smith, et al. *Phys. Rev. A*, vol. 59, no. 1, pp. R47–R50, Jan. 1999.
- [12] J. Zhang, et al. *Science* (80-), vol. 276, no. 5315, pp. 1097–1100, 1997.
- [13] P. V. Nickles, et al. *Phys. Rev. Lett.*, vol. 78, no. 14, pp. 2748–2751, Apr. 1997.
- [14] J. Dunn, et al. *Phys. Rev. Lett.*, vol. 84, no. 21, pp. 4834–4837, May 2000.
- [15] R. Keenan, et al. *Phys. Rev. Lett.*, vol. 94, no. 10, p. 103901, Mar. 2005.
- [16] B. M. Luther, et al. *Opt. Lett.*, vol. 30 2, pp. 165–167, 2005.
- [17] Y. Wang, et al. *Phys. Rev. A*, vol. 72, no. 5, p. 53807, Nov. 2005.
- [18] B. A. Reagan, et al. *Phys. Rev. A*, vol. 89, no. 5, p. 53820, May 2014.
- [19] C. Baumgarten, et al. *Opt. Lett.*, vol. 41, no. 14, pp. 3339–3342, Jul. 2016.
- [20] D. Alessi, et al. *Phys. Rev. X*, vol. 1, no. 2, p. 21023, Dec. 2011.
- [21] F. Balmer, et al. “X-Ray Lasers 2012,” in *X-Ray Lasers 2012*, 2014, p. 147 Cha5.
- [22] H. Daido, et al. *Phys. Rev. Lett.*, vol. 75, no. 6, pp. 1074–1077, Aug. 1995.
- [23] Y. Wang, et al. *Opt. Lett.*, vol. 42, no. 19, pp. 3828–3831, Oct. 2017.
- [24] J. Crespo López-Urrutia, et al. *Proc SPIE*, pp. 258–264, 1994.
- [25] G. J. Tallents, et al. *AIP Conf. Proc.*, vol. 641, no. 1, pp. 291–297, 2002.
- [26] M.-C. Chou, et al. *Opt. Lett.*, vol. 34, no. 5, pp. 623–625, Mar. 2009.
- [27] H. Daido, “Review of soft X-ray laser researches and developments,” *Reports Prog. Phys.*, vol. 65, p. 1513, 2002.
- [28] B. J. MacGowan, et al. *Phys. Fluids B Plasma Phys.*, vol. 4, no. 7, pp. 2326–2337, 1992.